Available online at www.sciencedirect.com
ScienceDirect
Ceramics International 35 (2009) 763–769
CERAMICS INTERNATIONAL
www.elsevier.com/locate/ceramint

Effect of Pb excess in sol–gel process on phase composition in PFN ceramics

H. Bruncková *, L'. Medvecký, J. Mihalik, J. Ďurišin

Institute of Materials Research, Slovak Academy of Sciences, Watsonova 47, Košice 040 01, Slovak Republic

Received 2 January 2008; received in revised form 25 January 2008; accepted 16 February 2008
Available online 9 July 2008

Abstract

Lead iron niobate $Pb(Fe_{0.5}Nb_{0.5})O_3$ (PFN) precursors were prepared using sol–gel synthesis by mixing acetates Pb and Fe with Nb-ethylene glycol–tartarate (Pechini) complex at 80 °C and calcination of gels at 600 °C. Single pyrochlore phase with structure close to $Pb_3Nb_4O_{13}$ was formed in stoichiometric precursor and $Pb_3Nb_4O_{13}$ with small amount of perovskite phase $Pb(Fe_{0.5}Nb_{0.5})O_3$ in nonstoichiometric precursor prepared with the excess of Pb in molar ratio (Pb:Fe:Nb = 1.2:0.5:0.5). Average particle sizes of PFN calcined powders were ~120 nm. The metastable pyrochlore phase was partially decomposed to perovskite phase at sintering temperature of 1150 °C for 2, 4 and 6 h. Excess of Pb caused increasing of the density (7.4 g/cm^3) and content of the perovskite phase (~53 vol.%) in ceramics sintered for 4 h. In microstructures of PFN ceramics sintered at 1150 °C for different times, the bimodal grain size distribution was observed with small spherical grains of perovskite phase and larger octahedral grains, which represent the pyrochlore phase. Results of EDX analysis confirm that complex types of pyrochlore phases that differ in iron content were present in ceramics.

Keywords: A. Sintering; Pechini complex; Sol–gel; PFN precursor; Pyrochlore; Perovskite phase

1. Introduction

Lead-based complex perovskites with the general formula $A(B'B'')O_3$ such as $Pb(Mg_{1/3}Nb_{2/3})O_3$ (PMN) and $Pb(Fe_{1/2}Nb_{1/2})O_3$ (PFN) have received considerable attention since the late 1970s and have been applied recently in multilayer ceramic capacitors (MLCCs) and electrostrictive actuators [1–4]. Lead magnesium niobate PMN is a prototype relaxor ferroelectric compound most widely studied among lead-based complex perovskites. Meanwhile, solid solutions of lead iron niobate PFN and lead iron tungstate $Pb(Fe_{2/3}W_{1/3})O_3$ (PFW) were investigated for potential capacitor dielectrics [5,6].

It is very difficult to fabricate the pure perovskite (pv) ABO_3 PMN and PFN phases without the formation of the undesirable pyrochlore (py) $A_2B_2O_6$ phase, which degrades the physical properties of ceramics. To obtain single-phase PFN, four various synthesis techniques: basic process (conventional techniques) [7–9], double-step method (columbite [5]), wet chemical route [10,11] and molten salt synthesis [12]. In the conventional method (solid state reaction) the oxides (PbO, Fe_2O_3 and Nb_2O_5) are weighted and mixed under dry or wet conditions. Ananta and Thomas [7] developed two-stage mixed oxide synthetic routes for the preparation of single phase of lead-based PMN and PFN perovskites and two complex perovskite compounds at selected compositions in the PMN–PFN pseudo-binary system [5].

Besides, PFN is also synthetized by various wet chemical processing routes such as sol–gel [10], semi-wet hydroxide route [13] and coprecipitation [11,14–16]. Yoshikawa reported a chemical precipitation method for synthesis of PFN in 1996 [15]. In his work, niobium oxalate was introduced as Nb source and the stirring in the precipitation process was applied to realize the homogeneously distribution of metal ions in the precipitates [16]. The Pechini method is based on the formation of metallic complexes (Nb-complex) with carboxylic acid as ligand, normally citric or tartaric acid followed by a polymerization reaction with a polyalcohol (e.g. ethylene glycol) generating polyester. A colloidal sol–gel route represents the preparation of PMN–PFN systems from metal chlorides and nitrates whereas obtained powder precursors

* Corresponding author. Tel.: +421 55 7922455; fax: +421 55 7922408.
E-mail address: hbrunckova@imr.saske.sk (H. Bruncková).

0272-8842/$34.00
doi:10.1016/j.ceramint.2008.02.025

were calcined at 500 °C and sintered between 850 and 1150 °C [17]. Besides the sol–gel synthesis, the calcination temperature and pyrolysis conditions influence the formation of the final perovskite phase. Fine lead iron niobate powders with average particle size of 500 nm were prepared by the precipitation of Nb precursor in solution [11]. The formation perovskites PFN phases was emerged at a temperature as low as 400 °C and a pure perovskite was obtained at 800 °C.

The addition of PbO, which assisted densification and promoted grain growth through liquid phase sintering, adversely affected the dielectric properties using molten salt synthesis [12]. Excess of Pb in sol–gel process compensates the evaporation of PbO during sintering of PFN ceramics [10]. The pyrochlore phase is first formed at 500 °C and the perovskite phase begins to appear above 500 °C. A two phase is obtained at 700 °C and a nearly pure perovskite phase is formed at 750 °C. It is known that a stable pyrochlore phases are often created and they degrade physical properties in PFN ceramics. In PFN system, $Pb_3Nb_4O_{13}$, $PbFe_8O_{13}$, $Pb_2Fe_{1.2}Nb_{0.8}O_{5.5}$ and $Pb_3Fe_4Nb_4O_{21}$ pyrochlore phases were found with the major perovskite phase [18,19]. As the optimum sintering conditions (temperature and time), for the preparation of PFN ceramics using a mixed oxide route have been recommended lower temperature of 1175 °C for 2 h [18] and temperatures between 1050 and 1200 °C for 1 h in the case of PMN–PFN ceramics, or long sintering times up to 6 h were adopted [19].

The present paper describes the preparation of PFN ceramics using the sol–gel synthesis by mixing acetates Pb and Fe with Nb-ethylene glycol–tartarate complex. The influence of excess Pb on the phase composition and microstructure in the final PFN ceramics sintered at temperature of 1150 °C for different time was investigated.

2. Experimental

2.1. Preparation of PFN

The niobium precursor solution for $Pb(Fe_{0.5}Nb_{0.5})O_3$ (PFN) synthesis has been prepared by Pechini-type polymerizable complex method. The niobium chloride $NbCl_5$ was dissolved in ethanol C_2H_5OH and precipitated with ammonium NH_3 (aq) to prepare niobium oxide $Nb_2O_5{\cdot}xH_2O$. The Nb-tartarate-ethylene glycol (Pechini) complex was formed by a reaction of $Nb_2O_5{\cdot}xH_2O$ with tartaric acid (TA) and H_2O_2. The obtained solution was dried at 80 °C and dissolved in ethylene glycol (EG, the molar ratio of EG/TA = 5.5). PFN ceramics was prepared by the sol–gel synthesis according to diagram in Fig. 1. Lead acetate trihydrate $Pb(OAc)_2{\cdot}3H_2O$ and iron nitrate $Fe(NO)_3{\cdot}9H_2O$ were mixed in solvent acetic acid (AcOH) at 80 °C as lead and magnesium precursor solutions [20,21]. The molar ratio of PFN/AcOH in the solutions was kept at 1/5. The acetate solutions of Pb and Mg were mixed at 80 °C with the Pechini Nb-complex to obtain the organic mixtures (sols) with molar ratio of Pb:Fe:Nb = 1:0.5:0.5 or 1.2:0.5:0.5 (stoichiometric and non-stoichiometric PFN). Viscous PFN gels were calcined at 600 °C for 2 h in air after 12 h polycondensation of sols (at 25 °C) followed by drying at 100 °C for 8 h. After a uniaxial pressing

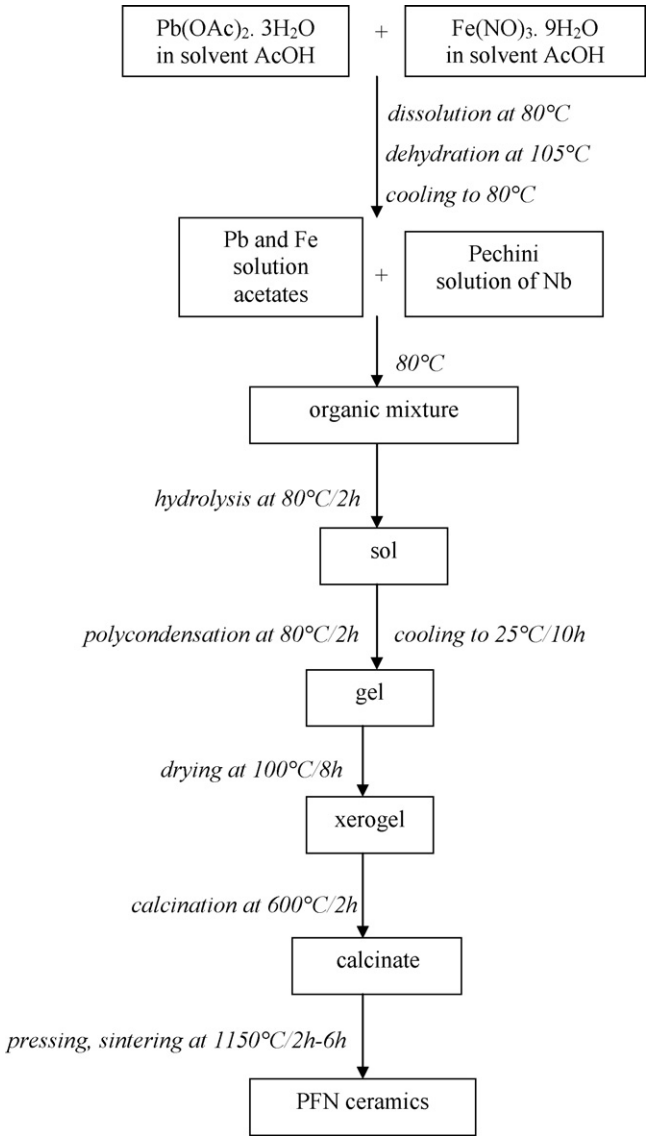

Fig. 1. A scheme for preparation of PFN ceramics by sol–gel synthesis using Pechini complex.

into tablet form, PFN precursors were sintered in air in closed crucible at the temperature of 1150 °C for 2, 4 and 6 h. Heating and cooling rate were ±5 °C/min.

2.2. Testing methods

The phase composition of PFN materials was analysed by the X-ray diffraction technique (XRD, a model Philips X Pert Pro) using Cu Kα radiation. The volume fraction of the perovskite phase in PFN systems (pv [vol.%]) can be calculated as a ratio of the intensities of XRD diffraction peaks from the reflection of (1 1 0) plane of pv phase (I_{pv}), reflection of (2 2 2) plane of pyrochlore phase (I_{py}) according to [22].

The size and morphology of powder particles were observed by a transmission electron microscopy (TEM, a model TESLA BS 500). The microstructures of the ceramic samples were characterized using a scanning electron microscope (SEM, a

Table 1
The properties (colors and efficiency w [wt.%]) of the $Pb(Fe_{0.5}Nb_{0.5})O_3$ (PFN) powders obtained sol–gel synthesis

Sample	Type of PFN	Mole ratio Pb:Fe:Nb	Sol at 80 °C	Gel at 25 °C	Dried gel at 100 °C	Powder at 600 °C	w[a] [wt.%]
1	Stoichiometric	1:0.5:0.5	Red	Orange	Green	Red	42
2	Nonstoichiometric	1.2:0.5:0.5	Brown	Yellow	Beige	Brown	48

[a] See text.

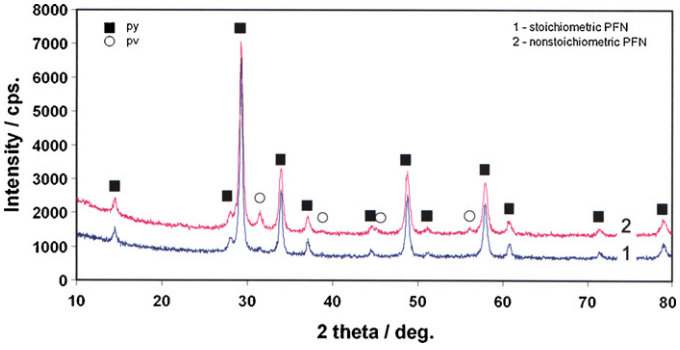

Fig. 2. XRD diffractograms of the PFN powders calcined at 600 °C: stoichiometric PFN (sample 1) and nonstoichiometric PFN (sample 2).

model TESLA BS 340) equipped with an energy dispersive X-ray (EDX) analyser LINK ISIS. The bulk densities of the final sintered ceramics were measured geometrically after polishing.

3. Results and discussion

3.1. PFN calcined powders

Using the sol–gel synthesis, two different types of $Pb(Fe_{0.5}Nb_{0.5})O_3$ (PFN) precursors were prepared with molar ratio of Pb:Fe:Nb = 1:0.5:0.5 or 1.2:0.5:0.5 (stoichiometric and nonstoichiometric PFN) (see Table 1). Table 1 summarizes the properties colors and efficiency of PFN powders (denoted as 1 and 2), where efficiency $w = (x/y) \times 100$, x is mass of obtained powder after calcination of gel and y is the theoretical mass of powder phase according to initial stoichiometry of PFN.

XRD diffractograms of calcined PFN powders (1 and 2) prepared at 600 °C are shown in Fig. 2. In the sample 1, the XRD patterns close to pure pyrochlore phase $Pb_3Nb_4O_{13}$ (JCPDS 25–443) and patterns characterize the trace amount of pv phase $Pb(Fe_{0.5}Nb_{0.5})O_3$ (JCPDS 32–522) were present only. The diffraction peak at 29.2° represents the reflection from (222) plane of py phase and peak at 31.5° – the line from diffraction of (1 1 0) plane of pv phase. In the sample 2, the pyrochlore phase $Pb_3Nb_4O_{13}$ with small amount perovskite phase (but higher than in sample 1) were present. A pyrochlore phase $Pb_2Fe_4Nb_4O_{21}$ and pv PFN phase were formed at 400 °C using coprecipitation synthesis of PFN powder [11]. Pure pv phase was obtained at 800 °C. A mixture of well-crystallized perovskite and metastable py phase was observed after calcination at 700 °C of PFN precursor obtained by sol–gel synthesis and complete transformation is achieved at 750 °C [10]. The SEM and TEM images of calcined powders (samples 1 and 2) are shown in Fig. 3a and b. The particles have almost spherical shape with the particle size between 100 and 130 nm in both PFN precursors. Excess of Pb caused in the powder with fine particles wrapped core-shell structure [11].

3.2. Stoichiometric and nonstoichiometric PFN ceramics

XRD diffractograms of the final PFN ceramics after sintering of precursors at 1150 °C for 2 and 6 h are shown in Fig. 4. In the sample 1 (Fig. 4a), both PFN perovskite phase with structure close to $Pb(Fe_{0.5}Nb_{0.5})O_3$ and pyrochlore ($Pb_3Nb_4O_{13}$ type) phase were present and the volume fraction of perovskite phase rapid decreased after sintering for 6 h (lower curve). In the sample 2 (Fig. 4b), the same types of perovskite and pyrochlore phases were found. The highest fraction of perovskite phase was observed in the nonstoichiometric ceramic sample at sintering time for 6 h (lower curve). Note that the formation of py phases such as $PbFe_8O_{13}$ (JCPDS 14–79) or $Pb_2Nb_2O_7$ (JCPDS 40–828) was not confirmed by XRD analysis.

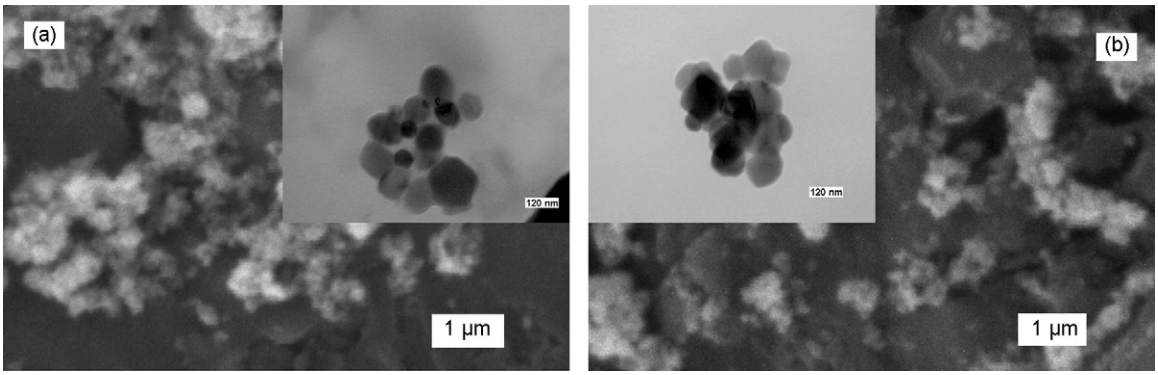

Fig. 3. REM and TEM micrographs of the calcined PFN powders: (a) stoichiometric (sample 1) and (b) nonstoichiometric (sample 2, bar (TEM micrographs) = 120 nm).

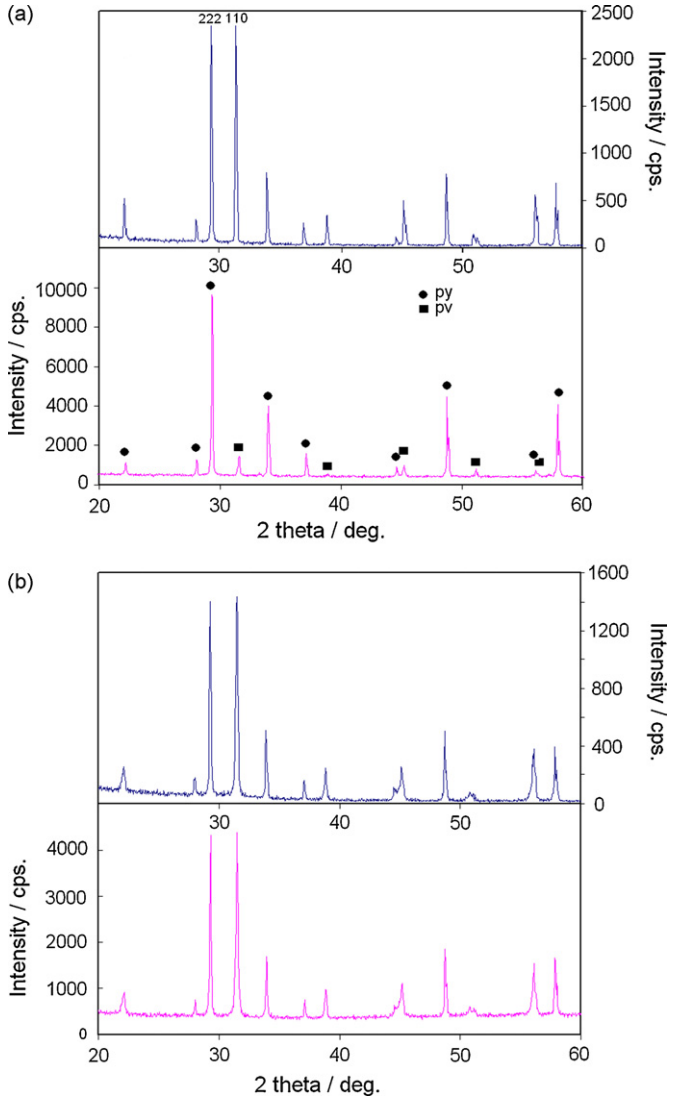

Fig. 4. XRD diffractograms of the PFN ceramics sintered at 1150 °C for 2 h (upper curves) and 6 h (lower curves): (a) stoichiometric and (b) nonstoichiometric.

Table 2 summarizes the volume fractions of pv phase in the ceramic samples and their densities as a function of sintering time at sintering temperature of 1150 °C. The content of pv phase in PFN samples was calculated according to [22]. In stoichiometric PFN powder composed from pure py phase (sample 1), the content of pv phase increased up to 51 vol.% after sintering at 1150 °C for 2 or 4 h, but it was found the rapid decrease in pv content down to ~16 vol.% after sintering for 6 h. The sintering time had only insignificant effect on the content of pv phase in nonstoichiometric PFN powder and the ceramic sample 2 contained approximately 50 vol.% of pv phase for each applied time. The maximum bulk density in sample 2 increased (from 6.5 to 7.4 g/cm^3) with sintering time up to 4 h and it decreased after sintering for 6 h, but the porosities were too high in both prepared ceramic samples. The optimum sintering time for the preparation of PFN ceramics at sintering temperature of

Table 2
The volume content of perovskite phase of PFN ceramics sintered at 1150 °C with different time for 2,4 and 6 h and the density ρ [g/cm^3] of polished pelets PFN ceramics

Sintering time [h]	pv phase [vol.%]			ρ [g/cm^3]		
	2	4	6	2	4	6
Sample						
1	50	51	16	5.1	6.0	5.7
2	50	53	50	6.5	7.4	4.9

1150 °C is 4 h from the point of view of the highest pv content in the samples. The maximum density (7.4 g/cm^3) was obtained in nonstoichiometric PFN ceramics at 1150 °C for 4 h. Effect 2 wt.% of PbO excess with on the densification of PFN powders in the temperature range 900–1000 °C for 4 h is described in [12]. For selected sintering temperatures, the densities of PFN ceramics with increasing amount of PbO excess were higher at temperatures of 900 and 950 °C than at 1150 °C.

Microstructures of fractured PFN ceramics sintered at the temperature of 1150 °C for 2, 4 and 6 h are shown in Fig. 5 obtaining from SEM. Spherical particles with average grain size around 4 μm and small fraction of particles with octahedral shape (≈4 μm size) were found in microstructure of stoichiometric ceramics after sintering for 2 h (Fig. 5a). In the microstructure, irregular pores with average size between 1 and 8 μm can be observed. The average size of octahedral grains, which represent the pyrochlore phase [18,19], was increased up to 7 μm after sintering for 4 h and higher fraction of very fine approximately 1 μm spherical grains probably perovskite phase [18,19] can be found in microstructure (Fig. 5b). Besides smaller pores with 3–4 μm size, large irregular pores (around 15 μm diameter) are clearly visible in ceramics. Microstructure ceramics sintered for 6 h significantly differs from previous microstructures (Fig. 5c). Large 20–25 μm irregular pores represent the main pore size fraction in ceramics and fine grains (≈1 μm size) were practically fully vanished from microstructure. Regular octahedral shaped grains with size between 3 and 7 μm can be seen and fraction of spherical particles (average grain size around 3 μm) was decreased in ceramics. In the microstructures of nonstoichiometric PFN ceramics sintered for selected times, coarse grains of pyrochlore phase with octahedral symmetry with average size of 5 μm and high fraction of small spherical shaped grains of 1 μm size were found (Fig. 5d–f). The large irregular pores with size up to 20 μm can be found in microstructures. Note that microstructures were practically the same in this type of ceramics. Grain size does not increase with sintering time in nonstoichiometric sample. PFN ceramics sintered at 1150 °C demonstrated porosity and well-crystallized irregular shaped grains [8]. The comparison between the microstructures of PFN ceramics sintered at 1000 °C for 4 h with 0 and 2 wt.% excess PbO showed that the grain size increased and the pores were eliminated with increasing amount of PbO [12]. In

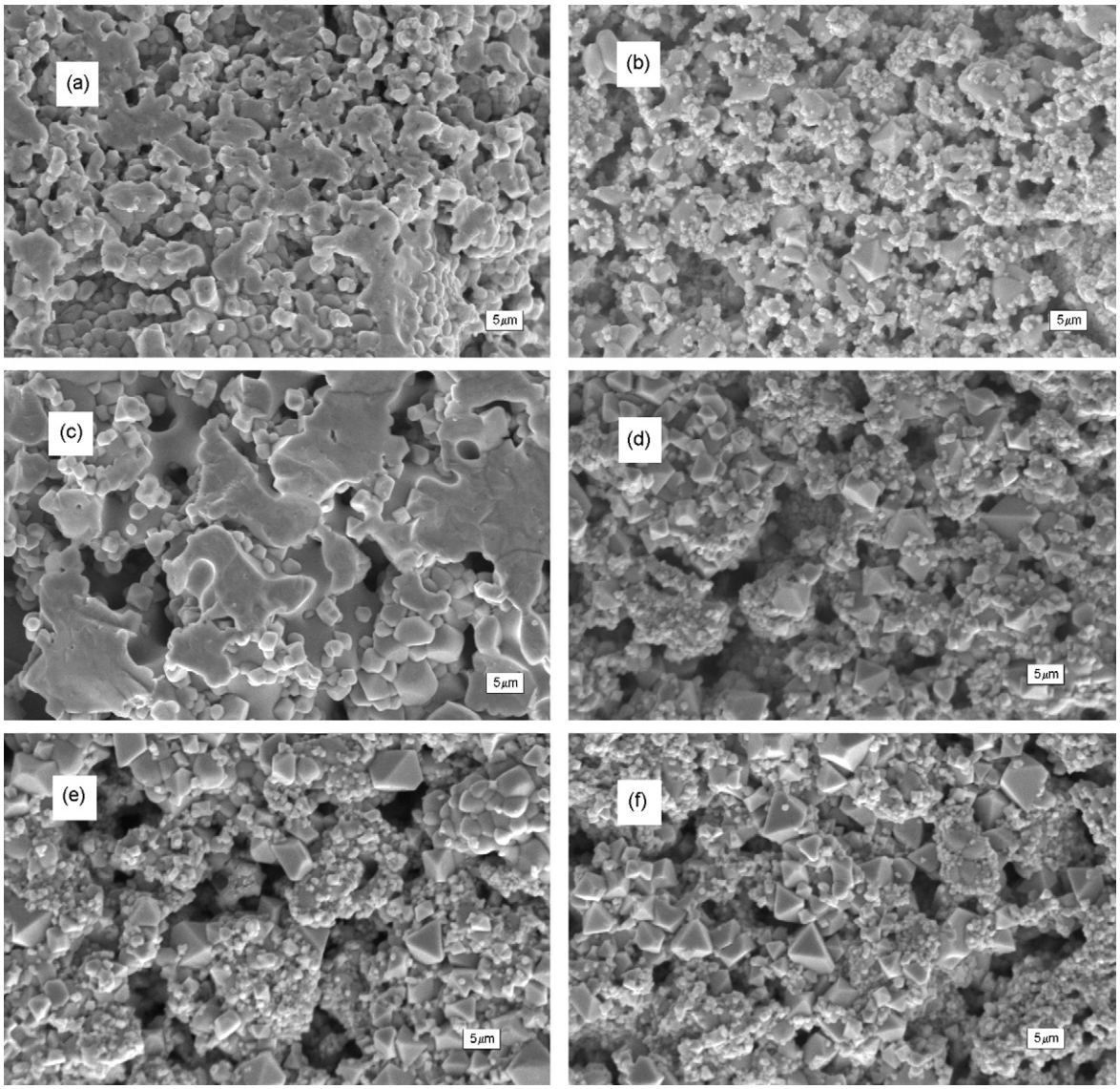

Fig. 5. SEM micrographs of fracture surfaces of the PFN ceramics sintered at the temperature of 1150 °C for 2, 4 and 6 h: (a–c) stoichiometric (sample 1) and (d–f) nonstoichiometric (sample 2).

ceramics, sintered at 1100 °C for 12 h the grain size did not increase with increasing amount of PbO.

The SEM micrographs of polished and etched PFN ceramic samples are shown in Fig. 6a and b. Two types of different phases are visible in both types of ceramics that are represented with darker region of regular shape and region in which grains are not clearly distinguished in microstructure. Form EDX analysis results that darker phases contain much higher amount of iron in comparison with the second phase which is mainly composed from niobium and lead with small amount of iron. As it is clear from EDX map in Fig. 6b, lead and niobium is very homogeneously distributed in ceramic microstructures and the content of these elements decreases in locations with high iron concentration – darker phases. Note, that the exact composition of phases (for example in phases with higher iron content) cannot be determined because excited volume may be spacious than volume of grain of given phase and emission from matrix can affect on EDX spectrum. The statistical analysis of the composition at different locations on surface of samples from EDX spectra verify that for example py phase with XRD patterns close to $Pb_3Nb_4O_{13}$ phase has more complex composition with some amount of iron in lattice. We propose some small substitution Nb ions for Fe ions have not to change lattice parameters or XRD patterns of this phase because of similar ionic radiuses of Nb^{5+} and Fe^{3+} ions. From above result that complex types of py phases that differ in iron content such as $Pb_3Nb_{4-x}Fe_xO_y$, $PbNbFe_7O_y$ or $Pb_2Nb_{2-x}Fe_xO_y$ are present in samples.

Sintering time of 4 h at sintering temperature of 1150 °C represents optimal time for the transformation pyrochlore phases in PFN powders to the perovskite phase. Maximal densities in final ceramics were found for sintering time of 4 h.

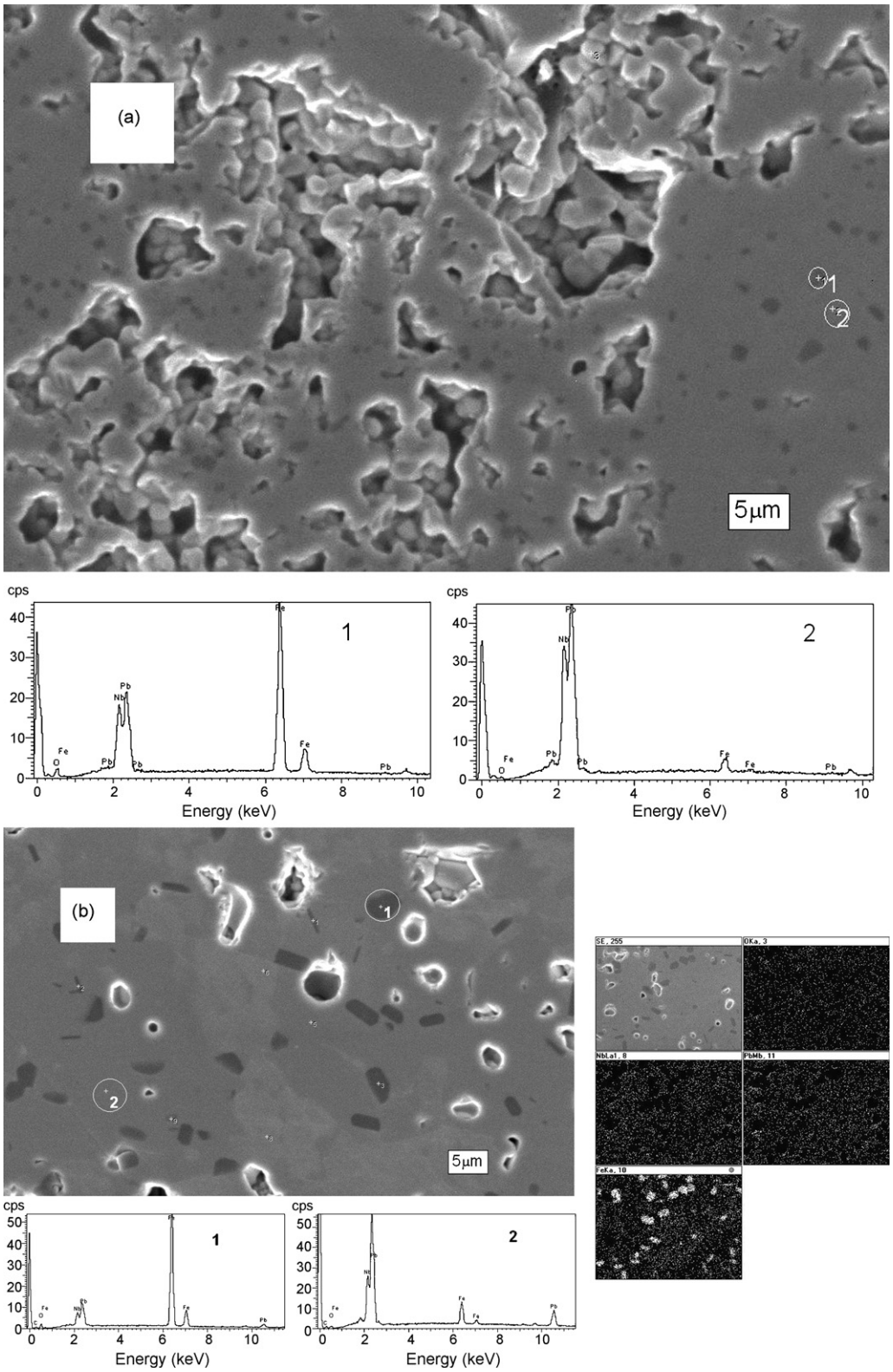

Fig. 6. SEM micrographs of polished and etched surface of PFN ceramics sintered at 1150 °C for 4 h: (a) stoichiometric (sample 1) with EDX analysis from different places (1 and 2) and (b) nonstoichiometric (sample 2) with EDX analysis from different places (1 and 2) and EDX map.

4. Conclusion

$Pb(Fe_{0.5}Nb_{0.5})O_3$ (PFN) ceramics were prepared using sol–gel synthesis by mixing acetates Pb and Fe with Nb-ethylene glycol–tartarate (Pechini) complex at 80 °C, calcining of gels at 600 °C and sintering at temperature of 1150 °C for various times.

The pyrochlore phase with structure close to pure pyrochlore $Pb_3Nb_4O_{13}$ phase was created by the calcination of stoichio-

metric PFN gel. Nonstoichiometric gel with excess of Pb in molar ratio (Pb:Fe:Nb = 1.2:0.5:0.5) was transformed on two phase system with major pyrochlore $Pb_3Nb_4O_{13}$ phase and small amount of the perovskite $Pb(Fe_{0.5}Nb_{0.5})O_3$ phase. Average size of particles in PFN calcined powders was ∼120 nm.

Excess of Pb caused the increase of the content of the perovskite phase (∼50 vol.%) in PFN ceramics sintered at 1150 °C for long time (6 h) while the decrease in pv phase content was found in stoichiometric PFN ceramics (∼16 vol.%). From the point of view of perovskite phase content and densities, the optimum sintering time of PFN is 4 h.

In the microstructures of PFN ceramics sintered at 1150 °C, octahedral grains, which represent the pyrochlore phase and spherical grains of perovskite phase were found, but this fraction decreased after sintering for 6 h. The grain size did not rise with sintering time in microstructures of nostoichiometric ceramics.

The results of EDX analysis showed that complex types of pyrochlore phases that differ in iron content were present in ceramics.

Acknowledgement

This work was supported by the Grant Agency of the Slovak Academy of Sciences through project No. 2/0050/08.

References

[1] K. Uchino, S. Nomura, L.E. Cross, S.J. Jang, R.E. Newnham, J. Appl. Phys. 51 (1980) 1142.
[2] S.J. Jang, K. Uchino, S. Nomura, L.E. Cross, Ferroelectrics 27 (1980) 31.
[3] K. Uchino, Am. Ceram. Soc. Bull. 65 (1986) 647.
[4] S.L. Swartz, T.R. Shrout, W.A. Schulze, L.E. Cross, J. Am. Ceram. Soc. 67 (1984) 311.
[5] S.G. Jun, N.K. Kim, J.J. Kim, S.H. Cho, Mater. Lett. 34 (1998) 336.
[6] P.M. Vilarinho, J.L. Baptista, J. Eur. Ceram. Soc. 11 (1993) 407.
[7] S. Ananta, N.W. Thomas, J. Eur. Ceram. Soc. 19 (1999) 155.
[8] N.S. Almodovar, R. Font, J. Portelleses, O. Raymond, E. Martinez, J.M. Siqueiros, J. Mater. Sci. 30 (2003) 3085.
[9] X. Wang, Z. Gui, L. Li, X. Zhang, Mater. Lett. 20 (1994) 75.
[10] M. Jenhi, E.H.E. Ghadraoui, H. Balli, M.E. Aatmani, M. Rafiq, Annal. Chim. Sci. Mater. 23 (1998) 151.
[11] J. Tang, M. Zhu, T. Zhong, Y. Hou, H. Wang, H. Yan, Mater. Chem. Phys. 10 (2007) 475.
[12] C.H.C. Chiu, S.B. Desu, Mater. Sci. Eng. B 2 (1993) 26.
[13] D. Mohan, R. Prasad, S. Banerjee, Ceram. Int. 27 (2001) 243.
[14] M.M.A. Sekar, A. Halliyal, K.C. Patil, J. Mater. Res. 11 (1996) 1210.
[15] Y. Yoshikawa, J. Am. Ceram. Soc. 79 (9) (1996) 2417.
[16] P.A. Lessing, Ceram. Soc. Bull. 66 (5) (1989) 1002.
[17] A. Larbot, H. Bali, M. Rafiq, A. Julbe, C. Guizard, L. Cot, J. Non-Crystalline Solids 147–148 (1992) 74.
[18] S. Ananta, N.W. Thomas, J. Eur. Ceram. Soc. 19 (1999) 1873.
[19] S. Ananta, N.W. Thomas, J. Eur. Ceram. Soc. 19 (1999) 2917.
[20] H. Brunckova, L. Medvecky, J. Briancin, K. Saksl, Ceram. Int. 30 (2004) 453.
[21] H. Brunckova, L. Medvecky, Mihalik, J. Eur. Ceram. Soc. 28 (2008) 123.
[22] S.L. Swartz, T.R. Shrout, Mater. Res. Bull. 17 (1982) 1245.